

Morphology and Molecular Phylogeny of the Soil Ciliate *Anteholosticha rectangula* sp. nov. from King George Island, Maritime Antarctica

Jae-Ho JUNG^{1,3}, Kyung-Min PARK^{1,2}, Sanghee KIM¹

¹ Division of Life Sciences, Korea Polar Research Institute, Yeosu-gu, Incheon, South Korea; ² Department of Biological Sciences, Inha University, Incheon, South Korea; ³ Department of Biology, Gangneung-Wonju National University, Gangneung, South Korea

Abstract. The soil ciliate *Anteholosticha rectangula* nov. spec. was discovered on King George Island in maritime Antarctica. Morphology and the nuclear SSU rDNA sequence were used to describe and infer the phylogenetic position of the new species. *Anteholosticha rectangula* is morphologically similar to *A. bergeri* and *A. verrucosa*, differing primarily by the morphology of the nuclear apparatus and dorsal kineties, respectively. The morphological features of related species are compared and discussed to confirm the validity of the new species. Molecular phylogenetic tree supports the previously reported polyphyly of the genus *Anteholosticha*.

Key words: New species, protargol impregnation, polyphyly, SSU rDNA, taxonomy

INTRODUCTION

Extreme environmental constraints in Antarctica allow only microorganisms such as bacteria and protists, and the smallest animals like nematodes, rotifers, and tardigrades to survive as dominant organisms on land. Terrestrial protozoa in maritime Antarctica are suggested to be important soil organisms due to their high biomass and respiration (Davis 1981). Ciliates are one of the most species-rich groups within Protozoa, and live in a variety of habitats such as soil, freshwater, and seawater (Small and Lynn 1985). However, few

studies of ciliates in Antarctic terrestrial habitats have been performed (Foissner 1996). Moreover, the dispersal of ciliates in such ecosystems by human activity has been ignored (Foissner 2011).

About 70 ciliate species have been recorded from Antarctic soils to date (Foissner 1998). Among these, five species belonging to the genus *Anteholosticha* have been recorded (Hada 1964, 1967; Sudzuki 1979; Foissner 1996). *Anteholosticha* is one of the most species-rich groups within urostylids and consists of 39 species (Berger 2008, Li *et al.* 2011, Xu *et al.* 2011, Park *et al.* 2013, Huang *et al.* 2014). Over half of the species have terrestrial or freshwater habitats. All *Anteholosticha* species recorded in Antarctica were found in grass or moss. Species richness and abundance of terrestrial ciliates are influenced by habitat conditions such as soil type (e.g., fellfield, moss, ornithogenic soil) or moss species (Petz 1997, Mieczan and Tarkowska-Kukuryk 2014).

Address for correspondence: Sanghee Kim, Division of Life Sciences, Korea Polar Research Institute, 26 Songdomirae-ro, Yeosu-gu, Incheon 406-840, South Korea; Tel.: +82 32 760 5515; mob.: +82 10 2887 0752; Fax: +82 32 760 5509; E-mail: sangheekim@kopri.re.kr

In this study we discovered new ciliate from a surface soil layer partially covered by moss on King George Island in maritime Antarctica. Based on comparative morphology, we describe the new species *Anteholosticha rectangula*. Its phylogenetic position is inferred from analyses of the SSU rDNA sequence.

MATERIALS AND METHODS

Sample collection and identification

Anteholosticha rectangula nov. spec. was discovered from a surface layer soil sample taken on King George Island, Antarctica (S62°14'28.56" W58°44'52.88") in January 2013. Daily records of temperature were measured by the Automatic Meteorological Observation System (AMOS) at King Sejong Station on King George Island. The sample was transported to a laboratory at King Sejong Station on King George Island within few hours, dried at 60°C for 24 hours, and then stored at 4°C. After transferring the sample to the laboratory in South Korea, ciliates were reactivated at 4°C using the non-flooded Petri dish method (Foissner *et al.* 2002a, b).

Living specimens were observed first under a stereomicroscope (Leica M205 C, Leica Microsystems, Wetzlar, Germany) and an inverted microscope (Zeiss Axio Vert.A1, Carl Zeiss, Oberkochen, Germany), and then under brightfield and differential interference contrast (DIC) at magnifications of 50 × to 1000 × using a light microscope Zeiss Axio Imager2 (Carl Zeiss, Oberkochen, Germany). Protargol-impregnation following 'Procedure A' in Foissner (2014) was used to reveal details of the ciliature and nuclear apparatus. For the staining, the protargol powder was manually synthesized according to the method described by Pan *et al.* (2013).

General terminology follows Lynn (2008), and specific terms for *Anteholosticha* and urostyleids follow Berger (2006).

SSU rRNA gene sequencing

A single cell was isolated after individuals of *A. rectangula* were picked from the culture samples and transferred to distilled water several times using microcapillary. Genomic DNA was extracted using a RED-Extract-N-Amp Tissue PCR Kit (Sigma, St. Louis, MO, USA) in accordance with the manufacturer's instructions. The conditions for PCR were as follows: denaturation at 94°C for 3 min, followed by 40 cycles of denaturation at 95°C for 15 s, annealing at 58°C for 30 s, extension at 68°C for 4 min, and a final extension step at 72°C for 7 min. A nearly complete SSU rRNA gene was amplified using two primers: slightly modified New EukA (5'-CTG GTT GAT YCT GCC AGT-3') and LSUrev3 (5'-GCA TAG TTC ACC ATC TTT CG-3') (Sonnenberg *et al.* 2007). The PCR products were purified using a QIAquick® PCR Purification Kit (Qiagen, Hilden, Germany). Two internal primers were used for sequencing: 18S+810 and 18S-300 (Jung *et al.* 2011). DNA sequencing was performed using an ABI 3700 sequencer (Applied Biosystems, Foster City, CA, USA).

Molecular analyses

SSU rRNA gene sequences of 54 species were obtained from the NCBI database to analyze the phylogenetic position of *A. rect-*

angula (see Suppl. Table 1). *Diophrys appendiculata* was selected as the outgroup. GenBank accession numbers are shown after the species name in the phylogenetic tree. The sequences were aligned using ClustalX 1.81 (Jeanmougin *et al.* 1998) and manually trimmed at both ends in BioEdit 7.1.11 (Hall 1999). The alignment was then further refined by visual assessment. A best-fit substitution model for the phylogenetic analyses was chosen using the jModelTest 2.1.7 (Darriba *et al.* 2012). We selected the model GTR + I (0.5400) + G (0.5190) under the Akaike information criterion (AIC). The Bayesian inference tree was built using MrBayes 3.2.5 (Ronquist *et al.* 2012) with the Markov chain Monte Carlo (MCMC) for 1,000,000 generations with a burn-in of 300,000. PhyML version 20131022 (Guindon *et al.* 2010) in Bio-Linux 8 (Field *et al.* 2006) was used to infer maximum likelihood trees with 1,000 bootstrap replicates. Pairwise distances were calculated using Mega 5.2.2 (Tamura *et al.* 2011).

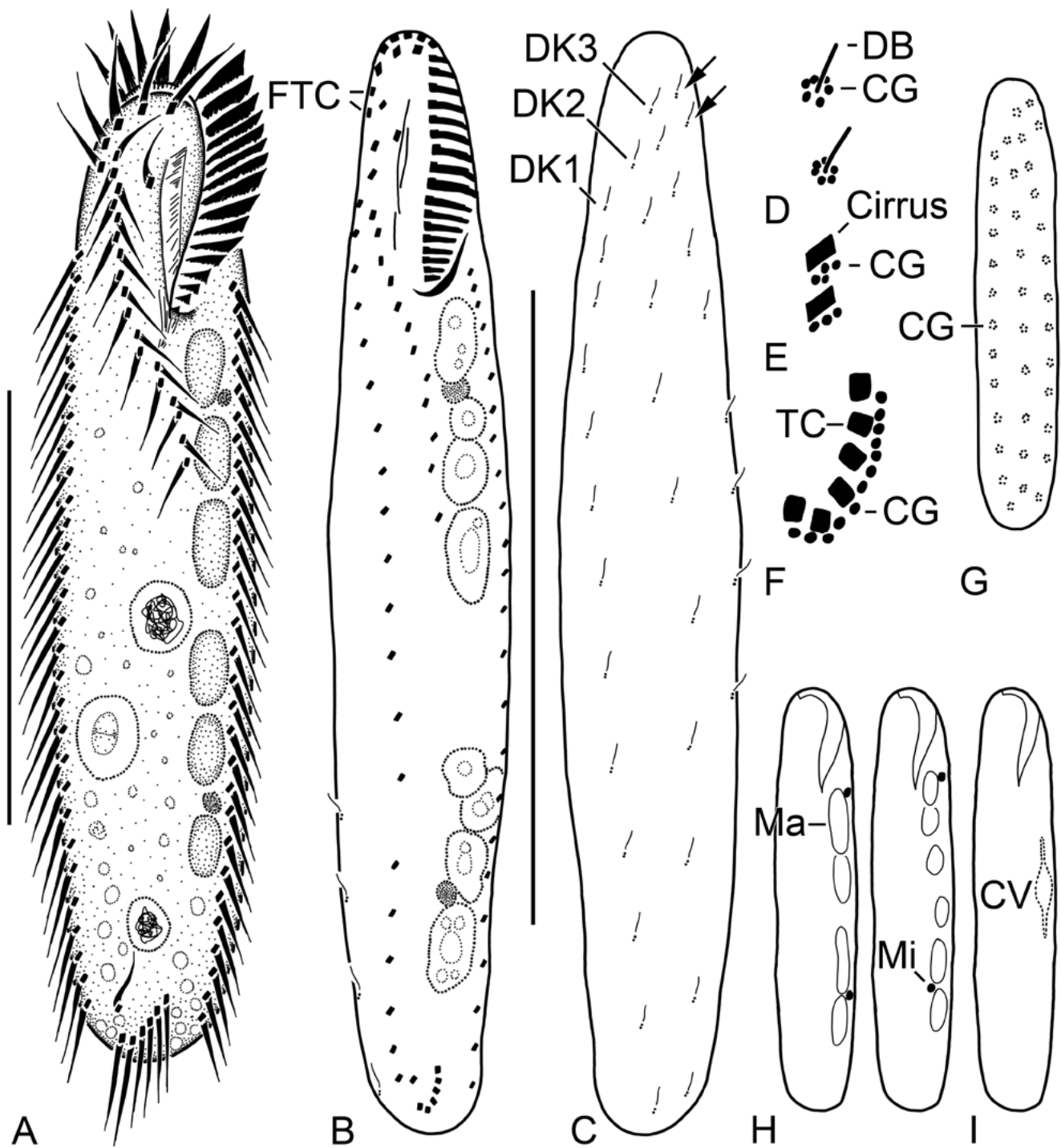
The approximately unbiased, weighted Shimodaira-Hasegawa, and weighted Kishino-Kasegawa tests was conducted to assess statistical significance of topological constraint, the monophyly of the genus *Anteholosticha*, using CONSEL ver. 0.20 (Shimodaira and Hasegawa 2001). The unconstrained (i.e., best) and the topologically constrained trees were inferred using the maximum likelihood criterion and a heuristic search with TBR branch swapping and 10 random sequence addition replicates in PAUP* v4.0b10 (Swofford 2003). The per-site log likelihoods of the unconstrained and constrained ML trees under the best-fit model (see above) were calculated using PAUP*. The monophyly of *Anteholosticha* as the constrained topology consisted of ten species of the genus: *A. gracilis*, *A. intermedia*, *A. manca*, *A. marimonilata*, *A. monilata*, *A. multicirrata*, *A. paramanca*, *A. pseudomonilata*, *A. pulchra*, and *A. rectangula* sp. nov.

RESULTS

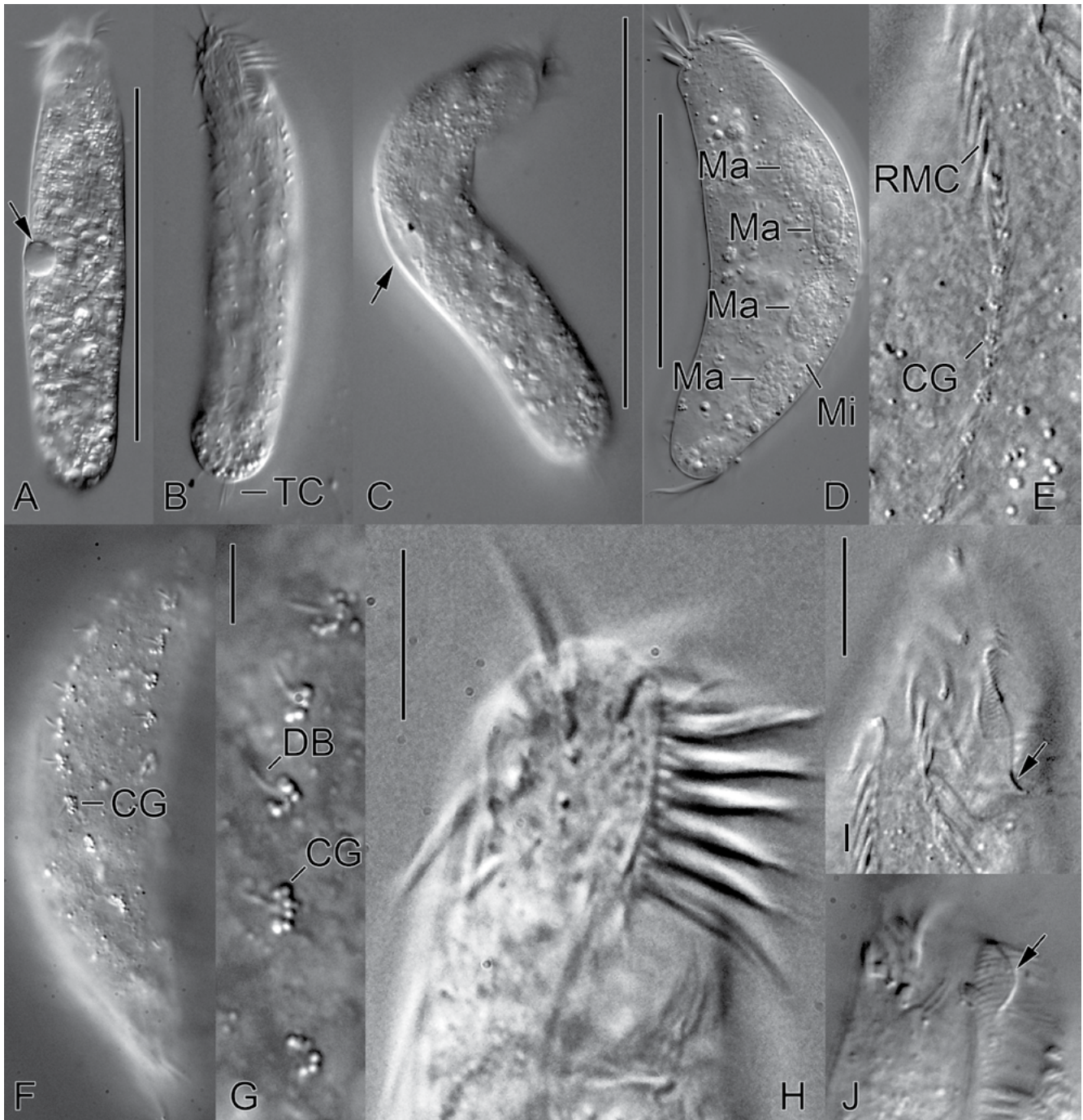
Description of *Anteholosticha rectangula* (Figs 1–3; Table 1)

Diagnosis: Size *in vivo* 70–140 × 20–30 μm. Body rectangular, colorless, flexible, and slightly contractile. Four to eight macronuclear nodules; two or three micronuclei. Contractile vacuole in left mid-body. Colorless cortical granules arranged along dorsal bristles and cirri; spherical to slightly ellipsoidal, 0.5–1.0 μm in diameter *in vivo*. On average 21 adoral membranelles, 24 right marginal, 25 left marginal, 18 midventral which terminates at about mid-body, and 7 transverse cirri. Invariably three frontal, one buccal, two frontoterminal, and one pretransverse cirri. Three bipolar dorsal kineties with two dikinetids in front of the right marginal cirral row. Caudal cirri lacking.

Type locality: Surface soil layer partially covered by moss, King George Island, maritime Antarctica (S62°14'28.56" W58°44'52.88"). Daily records of temperature showed a range of 2.4–6.5°C in January 2013.



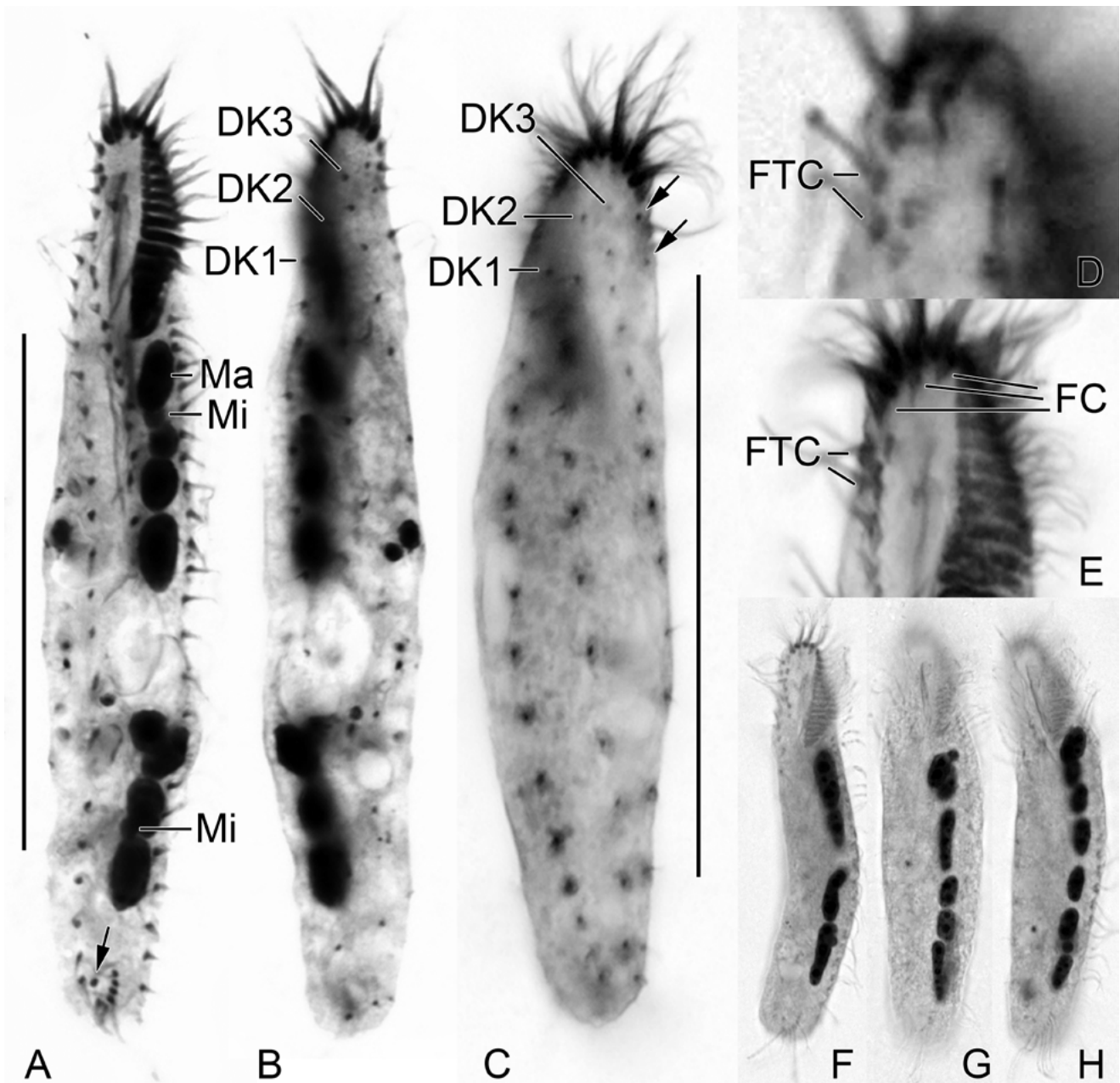
Figs 1A–I. Drawings of *Anteholosticha rectangulara* *in vivo* (A, D–G, I) and after protargol impregnation (B, C, H). **A** – ventral view of a representative specimen; **B** and **C** – ventral and dorsal views of holotype, arrows show two dikinetids; **D–G** – cortical granules on dorsal (D, G) and ventral sides (E, F); **H** – nuclear apparatus, showing variation in number and morphology; **I** – contractile vacuole. CG – cortical granules, CV – contractile vacuole, DB – dorsal bristles, DK1–3 – dorsal kineties 1–3, FTC – frontoterminal cirri, Ma – macronuclear nodules, Mi – micronuclei, TC – transverse cirri. Scale bars: 50 μ m.



Figs 2A–J. Photomicrographs of *Anteholosticha rectangula* *in vivo*. **A–C** – representative individuals showing contractile vacuole (arrows) and ciliatures; **D** – nuclear apparatus, **E–G** – cortical granules in ventral (**E**) and dorsal (**F**, **G**) views; **H–J** – ventral views showing oral apparatus; arrows in **I** and **J** show buccal lip and buccal seal, respectively. CG – cortical granules, DB – dorsal bristles, Ma – macronuclear nodules, Mi – micronuclei, RMC – right marginal cirri, TC – transverse cirri. Scale bars: 100 μ m (**A**, **C**, **D**), 5 μ m (**G**), 10 μ m (**H**, **I**).

Type material: One holotype slide (NIBR-PR0000106624) and two paratype slides (NIBR-PR0000106625, NIBRPR0000106626) including protar-

gol-stained specimens have been deposited in the National Institute of Biological Resources (NIBR), South Korea. Two additional paratype slides (ACNS000273,



Figs 3A–H. Photomicrographs of *Anteholosticha rectangula* after protargol impregnation. **A** and **B** – holotype specimen, ventral (**A**) and dorsal (**B**) view, arrow denotes pretransverse cirrus; **C** – dorsal view showing dorsal kineties, arrows denote two dikinetids anterior of right marginal cirral row; **D** and **E** – ventral views of anterior body showing buccal, frontal, frontoterminal, and midventral cirri; **F–H** – ventral views showing variation of the nuclear apparatus. DK1–3 – dorsal kineties 1–3, FC – frontal cirri, FTC – frontoterminal cirri, Ma – macro-nuclear nodules, Mi – micronuclei. Scale bars: 50 μ m.

ACNS000274) of the protargol-stained specimens have been deposited in the Korea Polar Research Institute (KOPRI). Circles marked on the bottom of the slides indicate the relevant specimens. The SSU rDNA sequence of type population has been deposited in the GenBank under the accession number KU175624.

Etymology: The species-group name *rectangula* refers to the rectangular body shape *in vivo*.

Description: Size *in vivo* 70–140 \times 20–30 μ m (Figs 1A; 2A–C); 67–95 \times 9–19 μ m after protargol impregnation (Figs 1B, C; 3A–C). Rectangular body outline *in vivo*, left and right cell margins almost parallel (Figs

Table 1. Morphometric data for *Anteholosticha rectangula*

Characteristic (stained)	N	Mean	SD	SE	CV	Min	M	Max
Body length, μm	23	75.5	6.2	1.3	8.3	67.1	74.0	94.5
Body width, μm	22	16.3	2.2	0.5	13.8	9.4	16.6	19.4
Adoral zone length, μm	22	20.0	1.9	0.4	9.4	17.4	19.7	24.5
AM, number	22	20.7	0.9	0.2	4.3	19	21	22
Width of largest AM, μm	22	5.0	0.4	0.1	7.3	4.1	5.1	5.6
BC, number	21	1	0	0	0	1	1	1
FC, number	19	3	0	0	0	3	3	3
FTC, number	19	2	0	0	0	2	2	2
MC, number	14	18.5	2.3	0.6	12.3	15	18	23
PTC, number	20	1	0	0	0	1	1	1
TC, number	20	7.1	1.0	0.2	14.2	6	7	9
Posterior TC to body end, length, μm	22	2.6	0.6	0.1	23.6	1.5	2.7	4.1
LMC, number	19	24.9	2.0	0.5	8.0	22	25	30
RMC, number	19	24.2	2.8	0.6	11.6	21	24	31
DK, number	20	3	0	0	0	3	3	3
DB in DK1, number	11	12.7	1.6	0.5	12.2	11	13	16
DB in DK2, number	14	11.2	1.0	0.3	8.7	10	11	13
DB in DK3, number	15	13	1.1	0.3	8.7	11	13	15
DB ahead of anterior RMC, number	20	2	0	0	0	2	2	2
Ma length, anteriormost, μm	22	8.5	1.8	0.4	21.0	5.5	9.1	10.9
Ma width, anteriormost, μm	22	4.2	0.7	0.1	15.7	3.2	4.1	5.5
Ma, number	20	5.8	1.7	0.4	29.3	4	6	8
Mi length, anteriormost, μm	23	2.3	0.2	0.0	10.0	1.9	2.3	2.9
Mi width, anteriormost, μm	23	2.1	0.2	0.0	9.7	1.6	2.1	2.5
Mi, number	22	2.1	0.4	0.1	16.4	2	2	3

AM – adoral membranelles; BC – buccal cirrus; CV – coefficient of variation in %; DB – dorsal bristles; DK – dorsal kineties; FC – frontal cirri; FTC – frontoterminal cirri; LMC – left marginal cirri; M – median; Ma – macronuclear nodules; Max – maximum; MC – midventral cirri; Mi – micronuclei; Min – minimum; N – number of specimens examined; PTC – pretransverse cirrus; RMC – right marginal cirri; SD – standard deviation; SE – standard error of the arithmetic mean; TC – transverse cirri.

2A, B). Cell colorless to grayish at low magnification $< 100\times$. Nuclear apparatus invariably on left cell margin arranged in a longitudinal row (Figs 1B; 2D; 3A, F–H); four to eight, $6\text{--}11 \times 3\text{--}6 \mu\text{m}$, ellipsoidal to oblong, macronuclear nodules; two or three, $2\text{--}3 \times 2\text{--}3 \mu\text{m}$, roughly spherical, micronuclei; nuclear apparatus sometimes split into two parts because of the presence of a food vacuole (Figs 1B; 3A). Contractile vacuole $10 \mu\text{m}$ in diameter when fully extended; located at left mid-body with collecting canals (Figs 1I; 2A, C). Colorless cortical granules roughly spherical, $0.5\text{--}1.0 \mu\text{m}$ in cross section; arranged around based of dorsal bristles (Figs 1D, G; 2F, G) and near cirri (Figs 1E, F; 2E). Cytoplasm colorless, with $5\text{--}10 \mu\text{m}$ -sized food

vacuoles usually located in posterior half of cell. Feeds on bacteria and small protists (e.g., diatoms).

Adoral zone of membranelles occupies approximately 25% of the body length (Fig. 3A); base of the largest membranelles about $5 \mu\text{m}$ long; cilia of the membranelles $15 \mu\text{m}$ long. Paroral and endoral membrane in parallel arrangement; endoral membrane commences at level of buccal cirrus (Figs 1B; 3A).

All cirri are relatively fine, generally $10\text{--}15 \mu\text{m}$ long *in vivo* (Figs 1A; 2B, H). Invariably three frontal, two frontoterminal, one buccal, and one pretransverse cirri. Midventral cirral pairs commence near frontoterminal cirri and terminate at nearly half of cell length; fifteen to twenty three cirri arranged in a zigzag pattern. Six

Table 2. Morphological attributes of species related to *Anteholosticha rectangularis*

	<i>A. bergeri</i> (three populations combined ^a)	<i>A. mancoidea</i>	<i>A. sigmoidea</i> (four populations combined ^a)	<i>A. sphagni</i>	<i>A. verrucosa</i> (two populations combined)	<i>A. rectangularis</i> nov. spec. (Antarctica)
Body length (stained), µm	49–82	120 (in life?)	50–98	60–90 (in life?)	46–90	67–95
Ma, number	13–34	usually 8	5–12	8–11	5–16	4–8
Mi, number	1–4	2 or 3	2 or 3	not known	1 or 2	2 or 3
CG	present, shiny pink	not known	present, colorless	absent	present, colorless to yellowish	present, colorless
AM, number	12–17	17–20 with gap	16–28	ca. 24 or 25	14–17	19–22
FC, number	3	4 (likely including cirrus III/2)	1–3	2	2 or 3	3
BC, number	1	1	1	1	1	1
FTC, number	2	2	2	not known	2	2
MC, number	11–15	ca. 7 cirral pairs	7–18 (left row), 8–18 (right row)	ca. 10 cirral pairs	7–15	15–23
PTC, number	1 or 2	2	1 or 2	2	not known, possibly 1 or 2 cirri included in TC	1
TC, number	3–5	5	3–6	ca. 5	2–4	6–9
LMC, number	13–28	17–19	16–35	24–27	12–18	22–30
RMC, number	10–27	16–20	15–33	23–26	13–21	21–31
DK, number	3	3	4	4	4	3
Habitat	terrestrial	freshwater	terrestrial	freshwater	likely terrestrial	terrestrial
Reference	Foissner (1987), Blatterer and Foissner (1988)	Hemberger (1985)	Foissner (1982), Foissner (1984)	Grolière (1975), Berger (2006)	Foissner (2000), Berger (2008)	this study

^a although some species might have sister taxa, all conspecific populations were combined because they are morphologically distinct from *A. rectangularis*.

AM – adoral membranelles; BC – buccal cirrus; CG – cortical granules; DK – dorsal kineties; FC – frontal cirri; FTC – frontoterminal cirri; LMC – left marginal cirri; Ma – macronuclear nodules; Mi – micronuclei; MC – midventral cirri; PTC – pretransverse cirri; RMC – right marginal cirri; TC – transverse cirri.

Table 3. Tree topology tests of the genus *Anteholosticha* with log likelihoods and *p*-values from approximately unbiased (AU), weighted Shimodaira-Hasegawa (WSH), and weighted Kishino-Hasegawa (WKH) tests on phylogenetic trees.

Topology	Log likelihood (-ln L)	Difference to best tree (-ln L)	AU (<i>p</i>)	WSH (<i>p</i>)	WKH (<i>p</i>)	Conclusion
Best maximum likelihood tree (unconstrained)	9,663.456		1.000	1.000	1.000	
Monophyly of <i>Anteholosticha</i>	10,054.531	391.075	6e-05	0.000	0.000	rejected

to nine transverse cirri which protrude beyond posterior end of body (Figs 1A; 2B; 3F–H). Right marginal row, composed of 24 cirri on average, commences near proximal end of endoral and terminates near pretransverse cirrus. Left marginal row, composed of 25 cirri on average, commences near proximal end of adoral zone of membranelles, and terminates near posterior end of right marginal row. Invariably three bipolar dorsal kineties with two dikinetids in front of right marginal cirral row (Fig. 1C, arrows), without any fragmentation; dorsal bristles 3 µm *in vivo*; dorsal kineties 1–3 composed of 11–16, 10–13, and 11–15 bristles, respectively. Caudal cirri lacking.

Occurrence and ecology: To date only at the type locality, King George Island. Moss-covered surface layer of soil.

Phylogenetic analyses: The SSU rDNA sequence of *A. rectangula* was 1,587 bp in length and, in the gene tree (Fig. 4), was nested within urostylids, clustering with some of its congeners (Holostichidae) and other two families, Pseudokeronopsidae and Pseudourostylidae. The 10 *Anteholosticha* species analyzed here were highly polyphyletic (see Table 3), and only 4 species showed a relatively close relationship to the new species (pairwise distances: *A. marimonilata* – 4.2%, *A. monilata* – 4.1%, *A. pseudomonilata* – 4.1%, *A. pulchra* – 5.4%). However, these five species (including *A. rectangula*) were not monophyletic.

DISCUSSION

Anteholosticha species reported in Antarctica:

Five species of *Anteholosticha* have been reported to date: 1) *A. bergeri* (Foissner, 1987) Berger, 2003 by Foissner (1996) from grass sward, Signy Island; 2) *A. intermedia* (Bergh, 1889) Berger, 2006 by Hada (1964) from moss, Langhovde, and Hada (1967) from ice blocks containing mosses and algae in pools and

wet beaches, Syowa station (Japan) and Mirny station (Russia); 3) *A. monilata* (Kahl, 1928) Berger, 2003 by Sudzuki (1979) from soil; 4) *A. multistilata* (Kahl, 1928) Berger, 2003 by Foissner (1996) from grass sward, Signy Island; and 5) *A. sigmoidea* (Foissner, 1982) Berger, 2003 by Foissner (1996) from moss and grass sward, Signy Island. Despite the infrequent study of Antarctic ciliates, the five Antarctic species of *Anteholosticha* were collected mainly from moss or grass implying that these environments provide a shelter for these species. In addition, the new species *A. rectangula* was discovered in the surface layer of soil partially covered by moss. Petz (1997) reported that a higher abundance and diversity of ciliates were recorded from moss samples than fellfield or ornithogenic soils. Moreover, different species richness of ciliates was recorded depending on the investigated moss species (Mieczan and Tarkowska-Kukuryk 2014). Although the genus *Anteholosticha* is one of the most species-rich hypotrich groups and more than half of the species occur in freshwater or terrestrial habitats (Berger 2006), few species are known to inhabit Antarctica. Further study is necessary to understand their ecological attributes and the limited occurrence in Antarctica.

Morphological comparison of *A. rectangula* and related species: The genus *Anteholosticha* is a species-rich group within urostylids, with 38 species listed in the Monograph of the Amphisiellidae and Trachelostylidae (Ciliophora, Hypotricha) (Berger 2008). Following the publication of Berger's monograph, three species were combined into new genera (e.g., *Arcuseries* Huang *et al.* 2014, *Nothoholosticha* Li *et al.* 2008), and four new species were assigned to *Anteholosticha* (e.g., *A. angida* Kumar, Kamra & Sapra, 2010, *A. marimonilata* Xu *et al.*, 2011, *A. multicirrata* Park, Jung & Min, 2013, *A. pseudomonilata* Li *et al.*, 2011). Consequently, 39 species are currently assigned to this genus.

The polyphyly of *Anteholosticha* is well known from SSU rDNA sequences (Park *et al.* 2013; Lv *et al.* 2015).

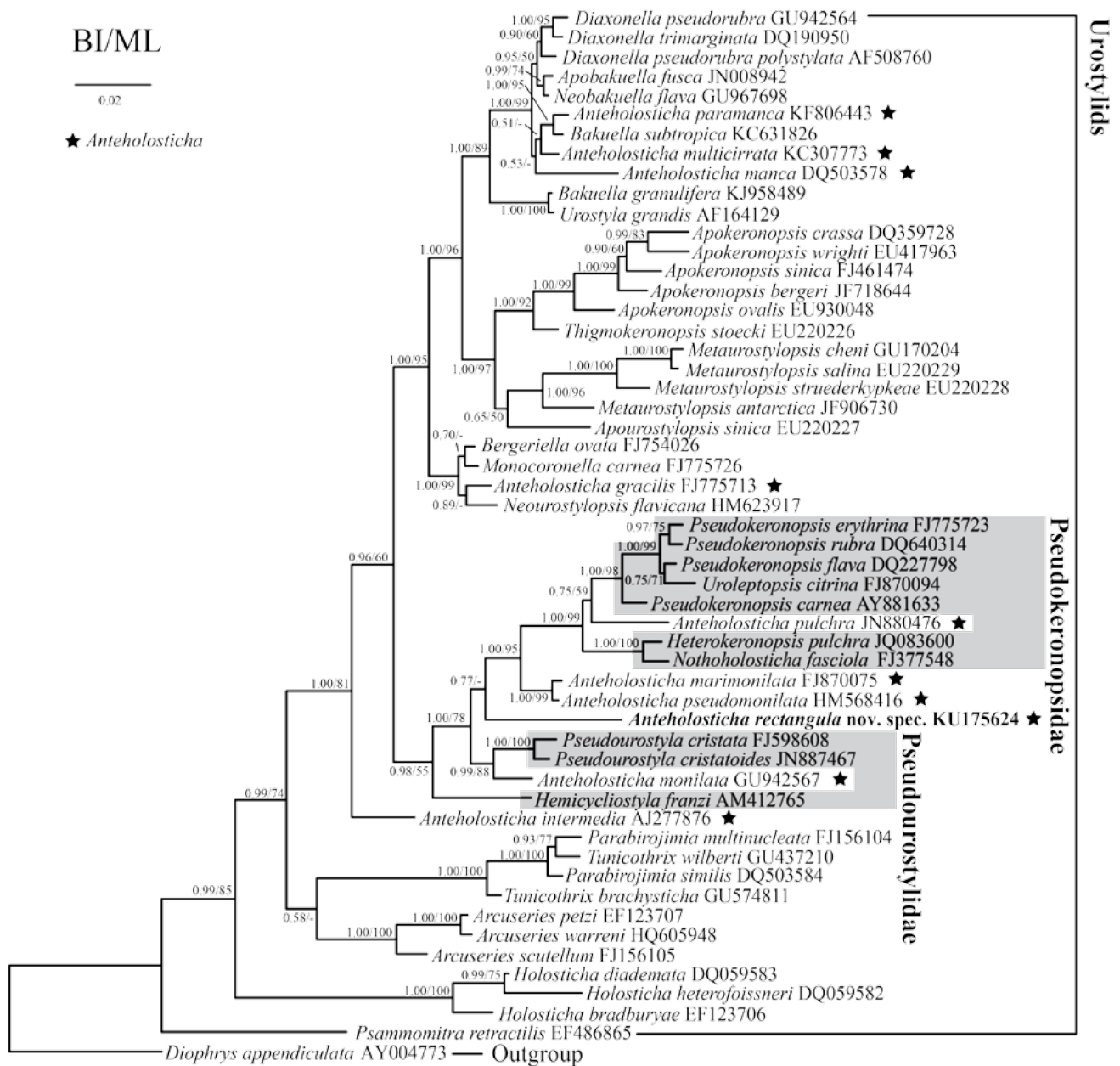


Fig. 4. Majority consensus tree from Bayesian inference using nuclear SSU rDNA sequences. *Anteholosticha rectangula* is indicated in bold in the tree. Posterior probabilities of Bayesian inference (BI) and bootstrap values of maximum likelihood (ML) are presented on each interior branch. Dashes denote a value showing less than half of the full posterior probability or bootstrap value. Scale bar indicates two base substitutions per one hundred nucleotides.

Mature cells of the congeners commonly have the following morphological attributes: three frontal cirri; buccal cirrus/cirri; midventral complex composed of cirral pairs only; one left and one right marginal cirral row; and transverse cirri (Berger 2006). The morphogenesis of *Anteholosticha* has been studied to attempt to resolve

the systematic problems and to be able to position new taxa appropriately (Li *et al.* 2008, Shao *et al.* 2011, Xu *et al.* 2011, Park *et al.* 2013). Park *et al.* (2013) analyzed 11 *Anteholosticha* species based on morphogenesis and the SSU rRNA gene, and split these species into seven types (I–VII). Of these, type VII, consisting of *A. petzi*,

A. scutellum, and *A. warreni*, was transferred to the new genus *Arcuseries* (Huang *et al.* 2014).

The new species *A. rectangula* matches the diagnosis of the genus *Anteholosticha* (Berger 2006). Of the 39 species in the genus, five are morphologically similar to *A. rectangula* in terms of body shape, size, and nuclear apparatus (i.e., more than 2 macronuclear nodules) (Table 2). In particular, *A. bergeri* (Foissner, 1987) Berger, 2003 and *A. verrucosa* (Foissner & Schade in Foissner, 2000) Berger, 2008 show greater morphological similarity of the cortical granulation than other species. However, *A. bergeri* differs from *A. rectangula* based on the macronuclear nodules (13–34 vs. 4–8 in number; scattered in the cytoplasm vs. arranged in a longitudinal row on the left side), adoral membranelles (12–17 vs. 19–22), transverse cirri (3–5 vs. 6–9), and cortical granules (shiny pink vs. colorless). *Anteholosticha verrucosa* can be distinguished from the new species by the adoral membranelles (14–17 vs. 19–22), transverse cirri including pretransverse cirri (2–4 vs. 7–10), and dorsal kineties (4 vs. 3). *Anteholosticha verrucosa* has fewer dorsal bristles in the dorsal kineties (DK) in each row (DK1 – 4 or 5, DK2 – 6–8, DK3 – 6–8, DK4 – 6 vs. DK1 – 11–16, DK2 – 10–13, DK3 – 11–15; bristle numbers in *A. verrucosa* counted from Foissner, 2000: Figs 87, 89).

Molecular phylogeny of *Anteholosticha rectangula*: The polyphyletic genus *Anteholosticha* consists of 40 species when the new taxon *A. rectangula* is included. However, the taxonomic descriptions of many species are incomplete, particularly regarding cortical granulation and dorsal kineties (Berger 2006). Moreover, the convergence (or plesiomorphy) of morphological attributes in mature cells hampers their systematic positioning within urostylids. As mentioned previously, Park *et al.* (2013) categorized the 11 species of *Anteholosticha* into seven types. However, the new species *A. rectangula* did not cluster with any of these types, and any other urostylids that showed a basal position in the clade consisted of type IV (*A. marimonilata*, *A. pseudomonilata*), type V (*A. pulchra*), and Pseudokeronopsidae. Although *A. bergeri* and *A. verrucosa* are morphologically similar to the new species, their SSU rDNA sequences are not available. Although the genus *Anteholosticha* is polyphyletic based on the SSU rDNA sequences, caution is required when interpreting phylogenetic trees because of misidentification of specimens in public databases. In addition, more genetic material of morphologically well-defined *Anteholosticha* specimens is required to accurately infer their phylogeny, especially for the terrestrial ciliates.

Acknowledgements. This study was supported by the Korea Polar Research Institute (research grants PE16020 and PM15040).

REFERENCES

- Berger H. (2006) Monograph of the Urostyloidea (Ciliophora, Hypotricha). *Monogr. Biol.* **85**: i–xv, 1–1303
- Berger H. (2008) Monograph of the Amphisiellidae and Trachelostylidae (Ciliophora, Hypotricha). *Monogr. Biol.* **88**: i–xvi, 1–737
- Blatterer H., Foissner W. (1988) Beitrag zur terricolen Ciliatenfauna (Protozoa: Ciliophora) Australiens. *Stapfia* **17**: 1–84
- Darriba D., Taboada G. L., Doallo R., Posada D. (2012) jModelTest 2: more models, new heuristics and parallel computing. *Nat. Methods* **9**: 772
- Davis R. C. (1981) Structure and function of two Antarctic terrestrial moss communities. *Ecological Monographs* **51**: 126–143
- Field D., Tiwari B., Booth T., Houten S., Swan D., Bertrand N., Thurston M. (2006) Open software for biologists: from famine to feast. *Nat. Biotechnol.* **24**: 801–803
- Foissner W. (1982) Ecology and taxonomy of the hypotrichida (Protozoa: Ciliophora) of some Austrian soil. *Arch. Protistenkd.* **126**: 19–143
- Foissner W. (1984) Infraciliatur, Silberliniensystem und Biometrie einiger neuer und wenig bekannter terrestrischer, limnischer und mariner Ciliaten (Protozoa: Ciliophora) aus den Klassen Kinetofragminophora, Colpodea und Polyhymenophora. *Stapfia* **12**: 1–165
- Foissner W. (1987) Neue und wenig bekannte hypotriche und colpodide Ciliaten (Protozoa: Ciliophora) aus Böden und Moosen. *Zool. Beitr. (N. F.)* **31**: 187–282
- Foissner W. (1996) Faunistics, taxonomy and ecology of moss and soil ciliates (Protozoa, Ciliophora) from Antarctica, with description of new species, including *Pleuroplitoides smithi* gen. n., sp. n. *Acta Protozool.* **35**: 95–123
- Foissner W. (1998) An updated compilation of world soil ciliates (Protozoa, Ciliophora), with ecological notes, new records, and descriptions of new species. *Eur. J. Protistol.* **34**: 195–235
- Foissner W. (2000) A compilation of soil and moss ciliates (Protozoa, Ciliophora) from Germany, with new records and descriptions of new and insufficiently known species. *Eur. J. Protistol.* **36**: 253–283
- Foissner W. (2011) Dispersal of protists: the role of cysts and human introductions. In: Biogeography of microscopic organisms: is everything small everywhere? (Eds. D. Fontaneto). Cambridge, U.K., Cambridge University Press, 61–87
- Foissner W. (2014) An update of 'basic light and scanning electron microscopic methods for taxonomic studies of ciliated protozoa'. *Int. J. Syst. Evol. Microbiol.* **64**: 271–292
- Foissner W., Agatha S., Berger H. (2002a) Soil ciliates (Protozoa, Ciliophora) from Namibia (Southwest Africa), with emphasis on two contrasting environments, the Etosha region and the Namib desert. Part I: Text and line drawings. *Denisia* **5**: 1–1063
- Foissner W., Agatha S., Berger H. (2002b) Soil ciliates (Protozoa, Ciliophora) from Namibia (Southwest Africa), with emphasis on two contrasting environments, the Etosha region and the Namib desert. Part II: Photographs. *Denisia* **5**: 1064–1459
- Grolière C.-A. (1975) Descriptions de quelques ciliés hypotriches des tourbières a sphaignes et des étendues d'eau acides. *Protistologica* **11**: 481–498
- Guindon S., Dufayard J. F., Lefort V., Anisimova M., Hordijk W., Gascuel O. (2010) New algorithms and methods to estimate

- maximum-likelihood phylogenies: Assessing the performance of PhyML 3.0. *Syst. Biol.* **59**: 307–321
- Hada Y. (1964) The fresh-water fauna of the Protozoa in the region of the Showa Station in Antarctica. *Bull. Suzugamine Women's Coll. Nat. Sci.* **11**: 5–21
- Hada Y. (1967) The fresh-water fauna of the protozoa in Antarctica. *Japanese Antarctic Research Expedition scientific reports. Special Issue 1*: 209–215
- Hall T. (1999) BioEdit: a user-friendly biological sequence alignment editor and analysis program for Windows 95/98/NT. *Nucleic Acids Symp. Ser.* **41**: 95–98
- Hemberger H. (1985) Neue Gattungen und Arten hypotricher Ciliaten. *Arch. Protistenkd.* **130**: 397–417
- Huang J., Chen Z., Song W., Berger H. (2014) Three-gene based phylogeny of the Urostyleoidea (Protista, Ciliophora, Hypotricha), with notes on classification of some core taxa. *Mol. Phylogenet. Evol.* **70**: 337–347
- Jeanmougin F., Thompson J. D., Gouy M., Higgins D. G., Gibson T. J. (1998) Multiple sequence alignment with Clustal X. *Trends Biochem. Sci.* **23**: 403–405
- Jung J.-H., Baek Y.-S., Kim S., Choi H.-G., Min G.-S. (2011) A new marine ciliate, *Metaurostylopsis antarctica* nov. spec. (Ciliophora, Urostyletida) from the Antarctic Ocean. *Acta Protozool.* **50**: 289–300
- Li L., Hu X., Alan W., Al-Rasheid K. A. S., Al-Farraj S. A., Shao C., Song W. (2008) Divisional morphogenesis in the marine ciliate *Anteholosticha manca* (Kahl, 1932) Berger, 2003 (Ciliophora: Urostyletida). *Acta Oceanol. Sin.* **27**: 157–163
- Li L., Khan S. N., Ji D., Shin M. K. (2011) Morphology and SSU rRNA gene sequence of the new brackish water ciliate, *Anteholosticha pseudomonilata* n. sp. (Ciliophora, Hypotrichida, Holostichidae) from Korea. *Zootaxa* **2739**: 51–59
- Lv Z., Shao C., Yi Z., Warren A. (2015) A molecular phylogenetic investigation of *Bakuella*, *Anteholosticha*, and *Caudiholosticha* (Protista, Ciliophora, Hypotrichia) based on three-gene sequences. *J. Eukaryot. Microbiol.* **62**: 391–399
- Mieczan T., Tarkowska-Kukuryk M. (2014) Ecology of moss dwelling ciliates from King George Island, Antarctic: the effect of environmental parameters. *Polish Polar Research* **35**: 609–625
- Pan X., Bourland W. A., Song W. (2013) Protargol Synthesis: An In-house Protocol. *J. Eukaryot. Microbiol.* **60**: 609–614
- Park K.-M., Jung J.-H., Min G.-S. (2013) Morphology, morphogenesis, and molecular phylogeny of *Anteholosticha multicirrata* n. sp. (Ciliophora, Spirotrichea) with a note on morphogenesis of *A. pulchra* (Kahl, 1932) Berger, 2003. *J. Eukaryot. Microbiol.* **60**: 564–577
- Petz W. (1997) Ecology of the active soil microfauna (Protozoa, Metazoa) of Wilkes Land, East Antarctica. *Polar Biol.* **18**: 33–44
- Ronquist F., Teslenko M., van der Mark P., Ayres D. L., Darling A., Höhna S., Larget B., Liu L., Suchard M. A., Huelsenbeck J. P. (2012) MrBayes 3.2: Efficient Bayesian phylogenetic inference and model choice across a large model space. *Syst. Biol.* **61**: 539–542
- Shao C., Gao F., Hu X., Al-Rasheid K. A., Warren A. (2011) Ontogeny and molecular phylogeny of a new marine urostyletid ciliate, *Anteholosticha petzi* n. sp. (Ciliophora, Urostyletida). *J. Eukaryot. Microbiol.* **58**: 254–265
- Shimodaira H., Hasegawa M. (2001) CONSEL: for assessing the confidence of phylogenetic tree selection. *Bioinformatics* **17**: 1246–1247
- Small E. B., Lynn D. H. (1985) Phylum Ciliophora Doflein, 1901. In: An illustrated guide to the protozoa, (Eds. J. J. Lee, S. H. Hutner, E. C. Bovee). Lawrence, Society of Protozoologists, 393–575
- Sonnenberg R., Nolte A. W., Tautz D. (2007) An evaluation of LSU rDNA D1-D2 sequences for their use in species identification. *Front. Zool.* **4**: 6
- Sudzuki M. (1979) On the microfauna of the Antarctic region III. Microbiota of the terrestrial interstices. *Mem. Nat. Inst. Polar Res., Tokyo Special Issue 11*: 104–126, Plates 1–10
- Swofford D. L. (2003) PAUP*. Phylogenetic analysis using parsimony (*and other methods). Ver. 4. Sinauer Associates, Sunderland, MA
- Tamura K., Peterson D., Peterson N., Stecher G., Nei M., Kumar S. (2011) MEGA5: Molecular evolutionary genetics analysis using maximum likelihood, evolutionary distance, and maximum parsimony methods. *Mol. Biol. Evol.* **28**: 2731–2739
- Xu Y., Huang J., Hu X., Al-Rasheid K. A. S., Song W., Warren A. (2011) Taxonomy, ontogeny and molecular phylogeny of *Anteholosticha marimonilata* spec. nov. (Ciliophora, Hypotrichida) from the Yellow Sea, China. *Int. J. Syst. Evol. Micr.* **61**: 2000–2014

Received on 13th July, 2015; revised on 1st December, 2015; accepted on 6th February, 2016

Suppl. Table 1. List of ciliate species analyzed using phylogenetic inference.

Species	Accession number	Species	Accession number
<i>Anteholosticha gracilis</i>	FJ775713	<i>Hemicycliostyla franzi</i>	AM412765
<i>Anteholosticha intermedia</i>	AJ277876	<i>Heterokeronopsis pulchra</i>	JQ083600
<i>Anteholosticha manca</i>	DQ503578	<i>Holosticha bradburyae</i>	EF123706
<i>Anteholosticha marimonilata</i>	FJ870075	<i>Holosticha diademata</i>	DQ059583
<i>Anteholosticha monilata</i>	GU942567	<i>Holosticha heterofoissneri</i>	DQ059582
<i>Anteholosticha multicirrata</i>	KC307773	<i>Metaurostyloopsis antarctica</i>	JF906730
<i>Anteholosticha paramanca</i>	KF806443	<i>Metaurostyloopsis cheni</i>	GU170204
<i>Anteholosticha pseudomonilata</i>	HM568416	<i>Metaurostyloopsis salina</i>	EU220229
<i>Anteholosticha pulchra</i>	JN880476	<i>Metaurostyloopsis struederkypkeae</i>	EU220228
<i>Anteholosticha rectangular nov. spec.</i>	KU175624	<i>Monocoronella carnea</i>	FJ775726
<i>Apobakuella fusca</i>	JN008942	<i>Neobakuella flava</i>	GU967698
<i>Apokeronopsis bergeri</i>	JF718644	<i>Neurostyloopsis flavicana</i>	HM623917
<i>Apokeronopsis crassa</i>	DQ359728	<i>Nothoholosticha fasciola</i>	FJ377548
<i>Apokeronopsis ovalis</i>	EU930048	<i>Parabirojimia multinucleata</i>	FJ156104
<i>Apokeronopsis sinica</i>	FJ461474	<i>Parabirojimia similis</i>	DQ503584
<i>Apokeronopsis wrighti</i>	EU417963	<i>Psammomitra retractilis</i>	EF486865
<i>Apourostyloopsis sinica</i>	EU220227	<i>Pseudokeronopsis carnea</i>	AY881633
<i>Arcuseries petzi</i>	EF123707	<i>Pseudokeronopsis erythrina</i>	FJ775723
<i>Arcuseries scutellum</i>	FJ156105	<i>Pseudokeronopsis flava</i>	DQ227798
<i>Arcuseries warreni</i>	HQ605948	<i>Pseudokeronopsis rubra</i>	DQ640314
<i>Bakuella granulifera</i>	KJ958489	<i>Pseudourostyla cristata</i>	FJ598608
<i>Bakuella subtropica</i>	KC631826	<i>Pseudourostyla cristatoides</i>	JN887467
<i>Bergeriella ovata</i>	FJ754026	<i>Thigmokeronopsis stoecki</i>	EU220226
<i>Diaxonella pseudorubra</i>	GU942564	<i>Tunicothrix brachysticha</i>	GU574811
<i>Diaxonella pseudorubra polystylata</i>	AF508760	<i>Tunicothrix wilberti</i>	GU437210
<i>Diaxonella trimarginata</i>	DQ190950	<i>Uroleptopsis citrina</i>	FJ870094
<i>Diophrys appendiculata</i>	AY004773	<i>Urostyla grandis</i>	AF164129